

# The onset of the fast dynamics in glassy polystyrene observed by the detrapping of guest molecules: a high-field Electron Paramagnetic Resonance study

V.BERCU<sup>1,2</sup>, M.MARTINELLI<sup>2</sup>, C.A. MASSA<sup>2</sup>, L.A. PARDI<sup>2</sup> and D.LEPORINI<sup>1,3</sup>

<sup>1</sup> *Dipartimento di Fisica “Enrico Fermi”, Largo B.Pontecorvo 3, I-56127 Pisa, Italy*

<sup>2</sup> *IPCF-CNR, via G.Moruzzi 1, I-56124 Pisa, Italy*

<sup>3</sup> *SOFT-INFM-CNR, P.zza A. Moro 2, I-00185, Roma, Italy*

PACS. 64.70.Pf – Glass transitions .

PACS. 76.30.-v – Electron paramagnetic resonance and relaxation.

PACS. 61.25.Hq – Macromolecular and polymer solutions; polymer melts; swelling .

**Abstract.** – The reorientation of the paramagnetic molecule TEMPO dissolved in glassy polystyrene ( PS ) is studied by high-field Electron Paramagnetic Resonance spectroscopy. Two different regimes separated by a crossover region are evidenced. Below 180K the rotational times are nearly temperature-independent with no apparent distribution. TEMPO is trapped. In the temperature range 180–220K a large increase of the rotational mobility is observed with widening of the distribution of correlation times which exhibits two components: i) a delta-like, temperature-independent component representing the fraction of TEMPO  $w$  still trapped; ii) a strongly temperature-dependent component representing the fraction of untrapped TEMPO  $1 - w$  undergoing activated motion over an exponential distribution of barrier heights. Above 180K a steep decrease of  $w$  is evidenced. The detrapping of TEMPO and the onset of its large increase of the rotational mobility at 180K are interpreted as signatures of the onset of the fast motion detected by neutron scattering at  $T_f = 175 \pm 25K$ .

*Introduction.* – The study of glassy solid dynamics is a very active one [1]. Particular interest and a current subject of strong controversy is the so called fast dynamics of glasses, occurring in the time window  $1-10^2 ps$  with several studies carried out mainly by neutron [2–6] and Raman scattering [7–10]. It is observed that on heating in a temperature range below  $T_g$  the dynamics of glass-forming systems deviates from the harmonic behavior and quasielastic scattering starts to accumulate in the low frequency range of the scattering function  $S(Q, \omega)$ . Accordingly, the temperature dependence of the atomic mean-squared displacement also starts to deviate from the linear dependence. We will denote by  $T_f$  the onset temperature above which the deviation from the harmonic behavior becomes it apparent.

The microscopic origin of the fast dynamics is still a question open to a strong controversy. Correlations of  $T_f$  with the so-called Vogel-Fulcher temperature  $T_0$  where the low-temperature extrapolation of the time scale of the  $\alpha$  relaxation diverges have been noted [3]. However, cases with  $T_f$  well below [4], equal [3], and well above [6]  $T_0$  are reported. The role of carbon-carbon torsional barriers to drive the fast dynamics of glass-forming polymers was also pointed out [2].

In the particular case of polystyrene ( PS ) of interest here,  $T_f$  was found to be  $175 \pm 25K$  [5] and  $200K$  [4], i.e. well below  $T_0 = 325K$ . **The measurements were carried out by neutron scattering and covered the time window  $\sim 1 - 10 ps$ .** For PS the onset of the fast motion has been ascribed to the change of the *librational* dynamics of the side-chain phenyl ring [4, 5] with expected involvement of the main-chain through the connecting bonds [11, 12]. In fact, the phenyl rings in glassy PS undergo very complex  $180^\circ$  flips and librational motions [11, 13] exploring several decades of characteristic times [12]. According to Nuclear Magnetic Resonance ( NMR ) the flip motion becomes frozen at about  $190K$  [14].

In glasses the dynamics is thermally activated in the substructures of the minima of the energy landscape [15]. Important information is drawn by the energy barrier distribution  $g(E)$  which is expected to be weakly temperature-dependent. The exponential shape of the energy-barriers distribution  $g(E)$  of the deep states of the energy landscape has been theoretically pointed out [16].

If the average trapping time  $\tau$  before to overcome the barrier of height  $E$  at temperature  $T$  is governed by the Arrhenius law,  $\tau = \tau_0 \exp(E/kT)$ ,  $k$  being the Boltzmann's constant, the distribution of barrier heights induces a distribution of trapping times  $\rho(\tau)$ . For gaussian  $g(E)$  with width  $\sigma_E$   $\rho(\tau)$  is the log-normal distribution ( LGD ) with width  $\sigma = \sigma_E/kT$ . If  $g(E)$  is exponential with width  $\bar{E}$

$$g(E) = \frac{1}{\bar{E}} \exp\left(-\frac{E}{\bar{E}}\right) \quad (1)$$

$\rho(\tau)$  is expressed by the power-law distribution ( PD )

$$\rho_{PD}(\tau) = \begin{cases} 0 & \text{if } \tau < \tau_{PD} \\ x\tau_{PD}^x \tau^{-(x+1)} & \text{if } \tau \geq \tau_{PD} \end{cases} \quad (2)$$

with  $x = kT/\bar{E}$ . If the width of the energy-barriers distribution is vanishingly small, a single trapping time ( SCT ) is found and  $\rho$  reduces to:

$$\rho_{SCT}(\tau) = \delta(\tau - \tau_{SCT}) \quad (3)$$

During the last few years high-field Electron Paramagnetic Resonance techniques ( HF-EPR ) were developed involving large polarizing magnetic fields, e.g.  $B_0 \cong 3T$  corresponding to Larmor frequencies of about  $95GHz$  ( W band ), [17, 18] or even larger [19–21]. HF-EPR is widely used in polymer science [21–24]. One major feature is the remarkable orientation resolution [24] due to increased magnitude of the anisotropic Zeeman interaction leading to a wider distribution of resonance frequencies [25]. **It is worthwhile that EPR is sensitive to the rotational dynamics in the range  $10^{-12} - 10^{-7}s$  and then spans the time scale of the fast dynamics of glasses and, in particular, the window covered by neutron scattering.**

In the present paper we present a detailed temperature study of the reorientation of a small probe molecule ( spin probe ) in glassy PS by using continuous-wave ( CW ) HF-EPR. Evidence is presented of a remarkable change of the rotational dynamics at  $\cong 180K$  which is interpreted as clear signature of the onset of fast dynamics of glassy PS.

In the next section the necessary background on EPR spectroscopy is outlined. Then, the results are presented and discussed.

*Background.* – The EPR signal is detected in paramagnetic systems. Since most polymers are diamagnetic, paramagnetic probe molecules ( spin probes ) are usually dissolved in

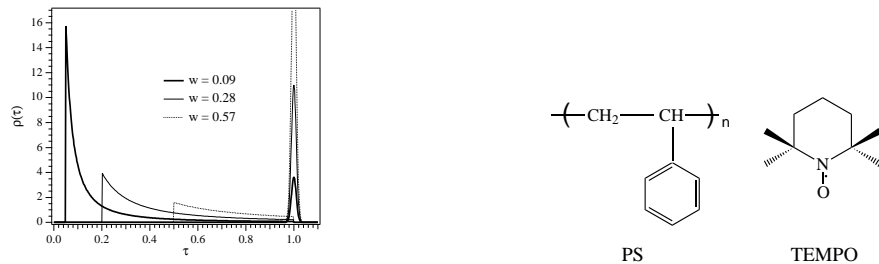


Fig. 1 – Left: schematic view of the bimodal distribution of correlation times  $\rho_{TPD}$  with  $\tau_{max} = 1$ ,  $x = 0.8$  and different values of the trapped fraction  $w$ . The delta function is replaced by a narrow gaussian with width 0.01. Right: chemical structures of PS and the spin probe TEMPO.

them. The EPR line shape of the spin probe is determined by the coupling between the reorientation of the latter and the relaxation of the electron magnetization  $\mathbf{M}$  via the anisotropy of the Zeeman and the hyperfine magnetic interactions. This yields a lineshape rich of informative spectral details [24, 25].

One important parameter to describe the rotational dynamics of the spin probe is the correlation time  $\tau_l$ , i.e. the area below the correlation function of the spherical harmonic  $Y_{l,0}$ . Because of the roughness of the energy landscape and the highly branched character of the free volume distribution, one expects that small spin probes undergo jump dynamics in glasses [26]. In the presence of jumps with finite size  $\phi$  correlations are lost roughly after one single trapping time, i.e.  $\tau_l \cong \tau$ . Then, in the presence of jump dynamics the distribution of the rotational correlation times  $\tau_l$  and the distribution of trapping times  $\tau$  of the spin probe do not differ too much. Henceforth, to emphasize that viewpoint,  $\tau_2$  will be denoted as  $\tau$ .

The occurrence of a static distribution of correlation times in glasses leads to evaluate the EPR line shape  $L(B_0)$ , which is usually detected by sweeping the static magnetic field  $B_0$  and displaying the first derivative, as a weighted superposition of different contributions:

$$L(B_0) = \int_0^\infty d\tau L(B_0, \tau) \rho(\tau) \quad (4)$$

where  $L(B_0, \tau)$  is the EPR line shape of the spin probes with correlation time  $\tau$  and  $\rho(\tau)$  is the  $\tau$  distribution. An efficient numerical method to calculate eq.4 is detailed elsewhere [22].

The identification of the rotational correlation time with the waiting time before one activated jump takes place, is questionable when the latter becomes extremely rare. In fact, if energy barriers are too high, entropic-like, alternative pathways become competitive to cancel orientation correlations. A simple account of that is provided by the truncation of  $\rho(\tau)$  in eq.4 beyond a certain  $\tau_{max}$  to give an effective distribution

$$\rho_T(\tau) = H(\tau_{max} - \tau)\rho(\tau) + w\delta(\tau - \tau_{max}) \quad (5)$$

where  $\delta(x)$  is the Dirac delta and  $H(x) = 1$  for  $x > 0$  and zero otherwise.  $\tau_{max}$  is expected nearly temperature-independent. The weight  $w$  is interpreted as the fraction of trapped molecules, i.e. the ones losing the rotational correlations by undergoing not-activated motion:

$$w = \int_{\tau_{max}}^\infty d\tau \rho(\tau) \quad (6)$$

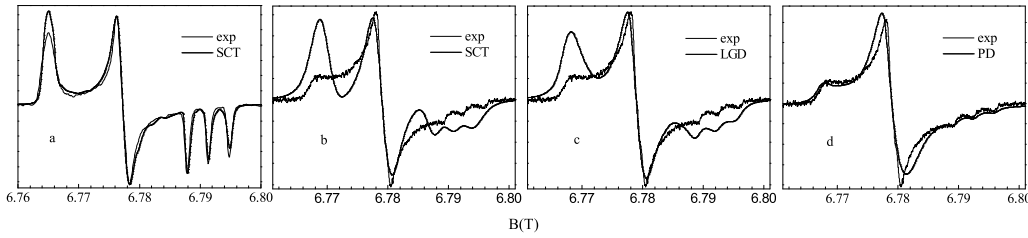


Fig. 2 – Comparison between the experimental HF-EPR lineshapes at  $190\text{GHz}$  ( thin lines ) and the best-fits by different models ( thick lines ). Panel a:  $T = 50\text{K}$ , SCT model ( eq.3 ) with  $\tau_{SCT} = 25\text{ns}$ . Jump angle  $\phi = 60^\circ$ . Nearly identical agreement is obtained by decreasing the jump angle down to  $\phi = 20^\circ$  with  $\tau_{SCT} = 102\text{ns}$ . Panel b:  $T = 270\text{K}$ , SCT model with  $\tau_{SCT} = 4.16\text{ns}$ . Jump angle  $\phi = 20^\circ$ . Panel c:  $T = 270\text{K}$ , LGD model with  $\tau_{LGD} = 3.6\text{ns}$ ,  $\sigma = 1$ . Jump angle  $\phi = 20^\circ$ . Panel d:  $T = 270\text{K}$ , PD model (eq.2 ) with  $\tau_{PD} = 0.22\text{ns}$ ,  $x = 0.57$ . Jump angle  $\phi = 20^\circ$ . TEMPO magnetic parameters are :  $g_x = 2.00994 \pm 3 \cdot 10^{-5}$ ,  $g_y = 2.00628 \pm 3 \cdot 10^{-5}$ ,  $g_z = 2.00212 \pm 3 \cdot 10^{-5}$ ,  $A_x(\text{mT}) = 0.62 \pm 0.02$ ,  $A_y(\text{mT}) = 0.70 \pm 0.02$ ,  $A_z(\text{mT}) = 3.40 \pm 0.02$ . The convolution by a gaussian with width  $0.15\text{mT}$  accounts for the inhomogeneous broadening.

Henceforth,  $\rho_{TPD}$  will denote  $\rho_T$  in the particular case  $\rho = \rho_{PD}$ , eq.2 with  $\tau_{PD} < \tau_{max}$ . Note that  $\rho_{TPD}$  depends on three parameters, e.g.  $x, w$  and  $\tau_{max}$ , being the fourth one, e.g.  $\tau_{PD}$ , being set by eq.6. Representative plots of  $\rho_{TPD}$  are shown in Fig.1.

To get information on the rotational dynamics of the spin probe one fits the experimental HF-EPR lineshapes collected at different temperatures and different operating frequencies ( in the present case  $190\text{GHz}$  and  $285\text{GHz}$  ) with the theoretical prediction as expressed via eq.4 and proper distribution function  $\rho_T$ , eq.5. It is worthwhile to list explicitly the number of adjustable parameters. They are divided in two sets: i) the parameters which are temperature- and frequency- independent. The set includes the six magnetic parameters of the spin probe ( the principal components of the  $g$  and hyperfine tensors ) and the jump angle  $\phi$ ; ii) the parameters which are temperature-dependent and almost frequency-independent. The set includes the width of the energy-barrier distribution, e.g.  $\overline{E}$  for the exponential distribution, eq.1, and the characteristic time scales of  $\rho_T$ , eq.5. In the case  $\rho_T = \rho_{TPD}$ , they are the shortest and the longest correlation time  $\tau_{PD}$  and  $\tau_{max}$  respectively. In the simplest case of no distribution of correlation times ( eq.3 )  $\tau_{SCT}$  only is adjusted.

*Results and discussion.* – The chemical structures of PS (  $M_w = 230\text{ kg mol}^{-1}$ ,  $M_w/M_n = 1.64$ ,  $T_g = 367\text{ K}$  ) and the spin probe TEMPO are shown in fig.1. Notice the strong similarity between TEMPO and the phenyl group of PS. TEMPO is stiff with average van der Waals radius  $3.3 \pm 0.2\text{\AA}$ . The spin probe was less than 0.08% in weight. The EPR experiments were carried out on the ultrawide-band EPR spectrometer operating at  $190\text{GHz}$  and  $285\text{GHz}$  which is detailed elsewhere [27]. The multi-frequency approach ensures better accuracy for determining the TEMPO dynamics.

Fig. 2 summarizes the findings of ref. [21] by showing the HF-EPR lineshape at  $190\text{GHz}$  of TEMPO in PS. The results at  $285\text{GHz}$  lead to the same conclusions [21]. It is seen that the lineshape at  $50\text{K}$  is well fitted by a *single* correlation time ( SCT model, eq.3, two adjustable parameters,  $\tau_{SCT}, \phi$  ). The small discrepancy between the simulation and the peak at low magnetic field was already noted [18]. The quality of the fit does not change if the jump angle  $\phi$  spans the range  $20^\circ - 60^\circ$ .

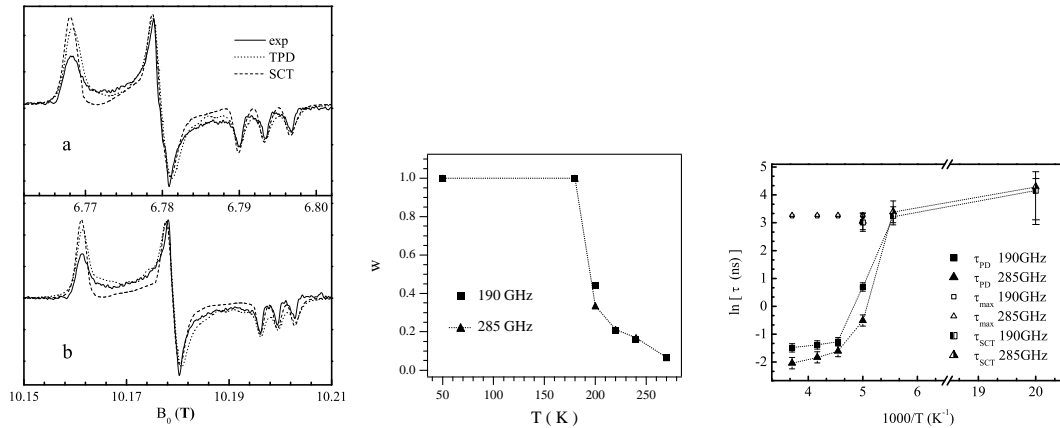


Fig. 3 – Left: The EPR line shape at  $T=200K$  and frequencies  $190GHz$  ( a ) and  $285GHz$  ( b ). The dotted lines are best-fit curves by using the TPD model ( eq.5 with  $\rho = \rho_{PD}$ , eq.2 with  $x = 0.32$ ,  $\tau_{PD} = 2ns$  ( a );  $x = 0.28$ ,  $\tau_{PD} = 0.6ns$  ( b ). For each frequency  $\tau_{max} = \tau_{SCT}$  at  $180K$  and  $\phi = 20^\circ$ . The fraction of trapped TEMPO molecules is  $w_{190GHz} = 0.44$  and  $w_{285GHz} = 0.34$ . The dashed lines are best-fit curves by using the SCT model with  $\phi = 20^\circ$ ,  $\tau_{SCT} = 20.3ns$  (panel a) and  $\tau_{SCT} = 21.2ns$  (panel b). Magnetic parameters of TEMPO and gaussian convolution as in fig.2. Center: temperature dependence of the trapped fraction of TEMPO molecules, eq.6 . Right: temperature dependence of the characteristic times of the SCT, PD and TPD distributions. The error bars at  $50K$  and  $180K$  account for the uncertainty on the best-fit value of the jump angle which is in the range  $20^\circ \leq \phi \leq 60^\circ$ ,  $20^\circ \leq \phi \leq 35^\circ$ , respectively . Dotted lines are guides for the eye.

Fig.2 also compares the best-fit of the lineshape at  $270K$  by the SCT model (eq.3, two adjustable parameters:  $\tau_{SCT}, \phi$ ), the PD model (eq.2, three adjustable parameters:  $\tau_{PD}, \phi$  and  $x$ ) and a model assuming the log-normal form of  $\rho(\tau)$  ( three adjustable parameters: the characteristic time  $\tau_{LGD}, \phi$  and  $\sigma$ ). After adjustment, it was found that the best-fit value of the jump angle for the three models was the same, i.e.  $\phi = 20^\circ$ . The better agreement by using  $\rho_{PD}$  is apparent.  $\rho_{PD}$  was proven to fit also the data at  $240K$  and provide the width of the exponential energy-barrier distribution  $\bar{E} = 600 \pm 36K$ , and  $\bar{E} = 705 \pm 42$  at  $190GHz$  and  $285GHz$ , respectively [21]. The exponential distribution of barrier-heights of PS  $g_{PS}(E)$  was evidenced also by internal friction [28], Raman [9] and light scattering [29]. The measured widths were  $\bar{E}_{IF}/k = 760 \pm 40K$ ,  $\bar{E}_{Raman}/k = 530 \pm 60K$  and  $\bar{E}_{LS}/k = 530 \pm 40K$ , respectively. By comparison, it is seen that the distribution of energy barriers  $g(E)$  probed by TEMPO is consistent with earlier data on PS taken by different techniques. It is worthwhile that both the exponential shape and the width of  $g_{PS}(E)$  manifest within the errors weak frequency-dependence in the wide range covered by the slow mechanic measurements carried out between  $1Hz - 87KHz$  [28] and the fast Raman and light scattering measurements data ( $\sim 3 - 300GHz$ ) [9, 29]. That invariance, which has been noted [30], is confirmed by the present HF-EPR measurements at  $190$  and  $285GHz$ .

**To summarize, two different rotational regimes of TEMPO were evidenced. At  $50K$  the reorientation of TEMPO exhibits a *single* correlation time whereas at  $240K$  and  $270K$  a *distribution* of correlation times is found. If one assumes that the distribution is due to activated jumps, one finds that TEMPO overcomes energy barriers whose distribution is consistent with PS one.**

To understand better the two regimes and the crossover region, first the low-

temperature regime was addressed. It is found that the EPR lineshapes at 190 and 285GHz are nicely fitted by the SCT model at 180K ( data not shown ) with negligible changes of the rotational rate  $\tau_{SCT}^{-1}$  with respect to 50K, see Fig. 3. The finding clarifies that in the temperature range 50 – 180K the reorientation of TEMPO: (i) is not activated and (ii) exhibits no distribution of rotational rates. This is interpreted by saying that at such low temperatures overcoming energy barriers is very difficult and entropic-like, alternative pathways become competitive to cancel orientation correlations, i.e. the representative point of TEMPO orientation is confined in "flat" regions of the energy landscape surrounded by high energy-barriers. From this respect, according to the discussion leading to eq.5, TEMPO is *trapped*, i.e.  $w = 1$ , eq.6. This must be contrasted with the effectiveness of the PD model at 240 and 270K pointing to  $\rho_T(\tau) \cong \rho(\tau) = \rho_{PD}$ , i.e. to a large detrapping of TEMPO ( $w \sim 0$ ).

The crossover region between the trapped and untrapped reorientation regimes of TEMPO has been also studied. On heating, first indications of the crossover are detected at 200K. Fig. 3 shows that the best-fit curve by using the SCT model deviates from the lineshapes at 190 and 285GHz of TEMPO at that temperature. Poor fits are obtained by the PD model as well. To improve the fit, the TPD model, which reduces to both the SCT and the PD models by setting  $w = 1$  and  $w = 0$  respectively, was considered.  $\rho_{TPD}(\tau)$  is truncated for  $\tau > \tau_{max}$ .  $\tau_{max}$ , i.e. the rotational correlation time of trapped TEMPO, was identified with  $\tau_{SCT}$  at 180K in all the fit procedures at temperatures  $T \geq 200K$ . Due to that,  $\rho_{TPD}(\tau)$  has the same adjustable parameters of  $\rho_{PD}(\tau)$ , eq.2, which, in turn, adds only *one* adjustable parameter to the one of the elementary SCT model, eq.3. Fig. 3 shows that the above strategy for the TPD model improves the fit at 200K and yields for the fraction of trapped TEMPO molecules  $w_{190GHz} = 0.44$  and  $w_{285GHz} = 0.34$ . The complete temperature dependence of the trapped fraction is presented in fig.3. It evidences a sharp decrease at 180 – 200K. Note that  $w$  is small at 270K, i.e.  $\rho_{PD} \cong \rho_{TPD}$  at that temperature, as expected. Fig.3 presents the overall temperature dependence of the characteristic times of the SCT ( $\tau_{SCT}$ ) and TPD ( $\tau_{PD}$  and  $\tau_{max}$ ) distributions. On heating, after a flat region between 50 – 180K, a drop of a factor of about 80 of the fastest timescale of TEMPO  $\tau_{PD}$  is evidenced between 180 – 220K. The drop parallels the strong decrease in the fraction of trapped TEMPO molecules  $w$ , fig.3. Interestingly, similar effects on guest molecules were reported. NMR showed that toluene ( similar in shape to TEMPO, see fig.1 ) in glassy PS exhibits both frozen and mobile components, the latter arising at  $\cong 170 - 180K$  ( after corrections for the PS plasticization due to the not small toluene concentration ) [14].

We interpret the drop in the fraction of trapped TEMPO molecules and the related accelerated dynamics which both set in at  $\cong 180K$  as signatures of the onset of the fast dynamics of PS which, according to neutron scattering studies, is located at  $T_f = 175 \pm 25K$  [5] and 200K [4] ( for better comparison with the present PS sample they should be read as 171K and 196K after corrections for the different  $T_g$  values ). Our results suggest the following scenario. Below 180K TEMPO molecules are unable to hop over barriers. The orientation correlations are lost by non-activated entropic-like processes with negligible distribution of the characteristic timescales. Above that temperature the onset of fast PS dynamics, which is well coupled to the rotational timescales of TEMPO, facilitates the crossover of the barriers which is successfully accomplished by a fraction  $(1 - w)$  of TEMPO molecules. Jumping over the barriers allows TEMPO to probe the exponential distribution of PS barrier-heights. As a consequence, a distribution of correlation times arises.

The onset of fast dynamics has been ascribed to the change of the *librational* dynamics of

the side-chain phenyl ring [4,5]. In fact, according to NMR the flip motion of the ring becomes frozen at about 190K [14]. Thus, it is tempting to conclude that the detrapping of TEMPO above 180K is due to the onset of some motion of the phenyl ring which is expectedly well coupled to TEMPO due to the similar shape ( see fig.1 ). However, the role of carbon-carbon torsional barriers to drive the fast dynamics of glass-forming polymers was also pointed out [2]. Additional work is needed to discriminate between these two views.

\* \* \*

J.Colmenero and A.P.Sokolov are gratefully acknowledged for helpful discussions.

## REFERENCES

- [1] C. A. Angell, K. L. Ngai, G. B. McKenna, P. F. McMillan, S. W. Martin, *J. Appl. Phys.* **88**, 3113 (2000).
- [2] J. Colmenero, A. Arbe, *Phys. Rev. B* **57**, 13508 (1998).
- [3] T. Kanaya, K. Kaji, *Adv. Polym. Sci.* **154**, 87 (2001).
- [4] T. Kanaya, T. Kawaguchi, K. Kaji, *J. Chem. Phys.* **104**, 3841 (1996).
- [5] B. Frick, U. Buchenau, and D. Richter, *Colloid Polym. Sci.* **273**, 413 (1995).
- [6] B. Frick, D. Richter, *Phys. Rev. B* **47**, 14795 (1993).
- [7] Y. Ding, V. N. Novikov, A. P. Sokolov, A. Cailliaux, C. Dalle-Ferrier, C. Alba-Simionesco, B. Frick, *Macromolecules* **37**, 9264 (2004).
- [8] V. N. Novikov, A. P. Sokolov, B. Strube, N. V. Surovtsev, E. Duval, A. Mermet, *J. Chem. Phys.* **107**, 1057 (1997).
- [9] A. P. Sokolov, V. N. Novikov, B. Strube, *Europhys. Lett.* **38**, 49 (1997).
- [10] A. P. Sokolov, U. Buchenau, W. Steffen, B. Frick, A. Wischnewski, *Phys. Rev. B* **52**, R9815 (1995).
- [11] J. Schaefer, M. D. Sefcik, E. O. Stejskal, R. A. McKay, *Macromolecules* **17**, 1107 (1984).
- [12] R. Khare, M. E. Paulaitis, *Macromolecules* **28**, 4495 (1995).
- [13] H. W. Spiess, *Colloid Polym. Sci.*, **261**, 193 (1983).
- [14] H. Sillescu, *Makromol. Chem., Macromol. Symp.* **1**, 39 (1986).
- [15] C. A. Angell, *Nature* **393**, 521 (1998).
- [16] C. Monthus, J. -P. Bouchaud, *J. Phys. A: Math. Gen.* **29**, 3847 (1996).
- [17] M. A. Ondar, O. Y. Grinberg, L. G. Oranskii, V. I. Kurochkin, Y. L. Lebedev, *J. Struct. Chem.* **22**, 626 (1981).
- [18] D. E. Budil, K. A. Earle and J. H. Freed, *J. Phys. Chem.* **97**, 1294 (1993).
- [19] T. N. Makarov, A. N. Savitsky, K. Mobius, D. Beckert, H. Paul, *J. Phys. Chem. A* **109**, 2254 (2005).
- [20] H. Blok, J. A. J. M. Disselhorst, S. B. Orlinkii, J. Schmidt, *J. Mag. Reson.* **166**, 92 (2004).
- [21] V. Bercu, M. Martinelli, C. A. Massa, L. A. Pardi, D. Loporini, *J. Phys.: Condens. Matter* **16** L479 (2004).
- [22] D. Loporini, X. X. Zhu, M. Krause, G. Jeschke, H. W. Spiess, *Macromolecules* **35**, 3977 (2002).
- [23] D. Loporini, V. Schädler, U. Wiesner, H. W. Spiess, G. Jeschke, *J. of Non-Crystalline Solids* **307 – 310**, 510 (2002).
- [24] D. Loporini, V. Schädler, U. Wiesner, H. W. Spiess, G. Jeschke, *J. Chem. Phys.* **119**, 11829 (2003).
- [25] *Biological magnetic resonance*, edited by L. J. Berliner and J. Reuben (Plenum, New York, 1989), Vol 8.
- [26] L. Andreozzi, F. Cianflone, C. Donati, D. Loporini, *J. Phys.: Condens. Matter* **8**, 3795 (1996).
- [27] G. Annino, M. Cassettari, M. Fittipaldi, L. Lenci, I. Longo, M. Martinelli, C. A. Massa and L. A. Pardi, *Appl. Magn. Reson.* **19**, 495 (2000).
- [28] K. A. Topp, D. G. Cahill, *Z. Phys. B* **101**, 235 (1996).
- [29] N. V. Surovtsev, J. A. H. Wiedersich, V. N. Novikov, E. Rössler, A. P. Sokolov, *Phys. Rev. B* **58**, 14888 (1998).
- [30] U. Buchenau, *Phys. Rev. B* **63** 104203 (2001).